Article

Activated Glassy Carbon Electrode as an Electrochemical Sensing Platform for the Determination of 4-Nitrophenol and Dopamine in Real Samples

Ali M. Abdel-Aziz, Hamdy H. Hassan, and Ibrahim H. A. Badr*

Read Online

ACCESS | 📊 Metrics & More | 📰 Article Recommendations | 🔲 Supporting Information

ABSTRACT: Glassy carbon electrode (GCE) was electrochemically activated using a repetitive cyclic voltammetric technique to develop an activated glassy carbon electrode (AGCE). The developed AGCE was optimized and utilized for the electrochemical assay of 4-nitrophenol (4-NP) and dopamine (DA). Cyclic voltammetry (CV) was employed to investigate the electrochemical behavior of the AGCE. Compared to the bare GCE, the developed AGCE exhibits a significant increase in redox peak currents of 4-NP and DA, which indicates that the AGCE significantly improves the electrocatalytic reduction of 4-NP and oxidation of DA. The electrochemical signature of the activation process could be directly associated with the formation of oxygen-containing surface functional groups (OxSFGs), which are the main reason for the improved electron transfer ability and the enhancement of the electrocatalytic activity of the AGCE. The effects of various parameters on the voltammetric responses of the AGCE toward 4-NP and DA were studied and optimized, including the pH, scan rate, and accumulation time. Differential pulse voltammetry (DPV) was also utilized to investigate the analytical performance of the AGCE sensing platform. The optimized AGCE exhibited linear responses over the concentration ranges of 0.04−65 μM and 65−370 μM toward 4-NP with a lower limit of detection (LOD) of 0.02 μM (S/N = 3). Additionally, the AGCE exhibited a linear responses over the concentration ranges of 0.02−1.0 and 1.0−100 μM toward DA with a lower limit of detection (LOD) of 0.01 μM (S/N = 3). Moreover, the developed AGCE-based 4-NP and DA sensors are distinguished by their high sensitivity, excellent selectivity, and repeatability. The developed sensors were successfully applied for the determination of 4-NP and DA in real samples with satisfactory recovery results.
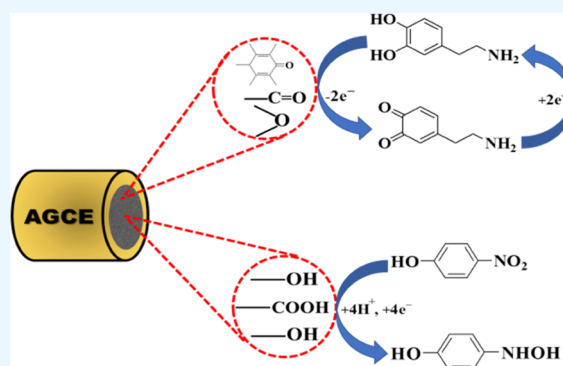
INTRODUCTION

Glassy carbon electrode (GCE) is favorable in electrocatalytic applications because of its remarkable properties such as low cost, excellent electrical conductivity, electrochemical inertness over a broad potential window, high hardness, chemical stability, impermeability, and ease of surface modification.[1,2] Activated glassy carbon electrodes (AGCEs) were shown to be one of the most interesting and widely applied modified electrodes in electrochemical research with improved electrocatalytic performance. Various activation procedures such as vacuum heating,[3] treatment with laser,[4] mechanical polishing,[5] ultrasonication,[6] and carbon arc[7] have been explored to enhance reversibility and electron transfer kinetics at the surface of the GCE. Moreover, electrochemical activation methods have also been reported, such as preanodization,[8−11] preanodization followed by short-time cathodization, and precathodization.[12,13] Recently, we showed that the GCE could be easily activated by anodization at a high potential (up to 2.5 V).[14] Such an anodization process at a high potential resulted in the formation of surface functional groups (SFGs). SFGs were shown to be the main reason for the improved

electron transfer ability and the enhancement of the electrocatalytic activity of the AGCE, which is advantageous in electrochemical sensors.[14] Our preliminary results showed that the AGCE could be used as a platform for the detection of oxidizable and reducible analytes.[14] Carboxylate and phenolate SFGs could facilitate the reduction of reducible analytes, and other SFGs (e.g., epoxide, quinone, and ketonic groups) could facilitate the oxidation of oxidizable analytes. Such SFGs facilitate the electron transfer at the AGCE surface, which results in the improvement of electron transfer and enhancement of the electrocatalytic activity. In this report, we have selected DA as a model for oxidizable analytes and 4-NP as a model for reducible analytes at the surface of the AGCE.
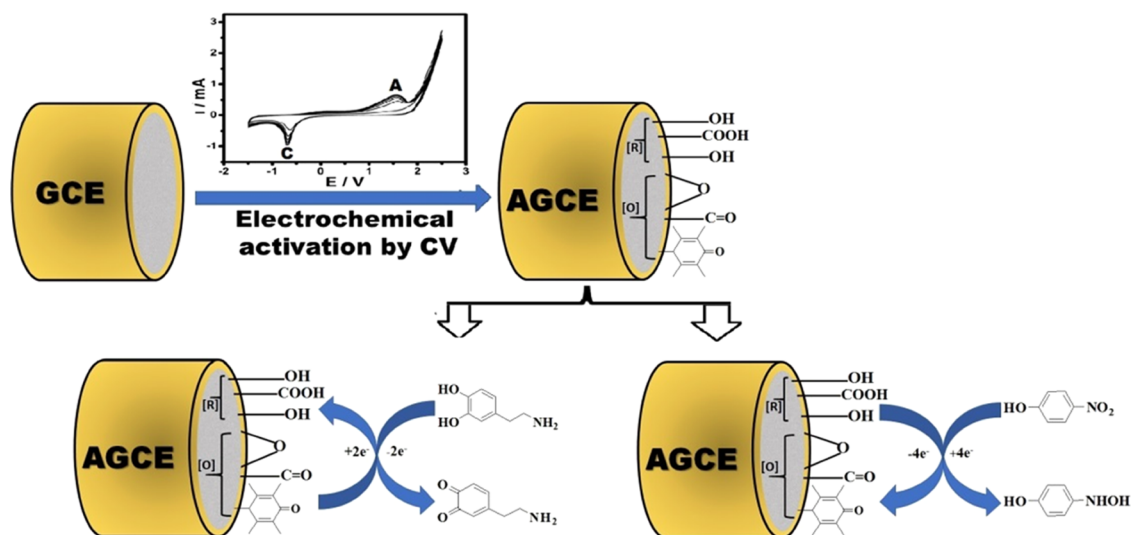
Scheme 1. Proposed Mechanism of Possible Redox Processes Occuring at the Surface of the AGCE

4-NP is extensively used in various industries[15,16] and may cause severe toxic effects on human beings, fish, animals, and plants.[17] The ingestion of 4-NP can cause health problems for humans and animals.[18] Because of these severe toxic effects, the US Environmental Protection Agency (EPA) listed 4-NP as a potential environmental pollutant. The European Union (EU) set the maximum allowed limit of 4-NP in drinking water at 0.43 μM.[16,19]

Dopamine (DA) is essential for the proper functioning of the cardiovascular, central nervous, renal, and hormonal systems.[20] Consequently, abnormal levels of DA may cause many neurological diseases (e.g., schizophrenia and cardiovascular and Parkinson's diseases).[21] Thus, the ability to develop rapid, safe, sensitive, selective, and environmentally friendly analytical methods for monitoring and detecting 4-NP and DA in real samples will have a crucial impact on human health and safety.

Various analytical methods for monitoring 4-NP and DA have been developed, including high-performance liquid chromatography,[22−24] gas chromatography-mass spectrometry,[25] chemiluminescence,[26−28] spectrophotometric methods,[29,30] electrophoresis,[31] surface plasmon resonance spectroscopy,[32] and fluorescence.[33−37] Even though these methods are superior in terms of sensitivity and accuracy, their rising cost, exhausting operations, laborious separation steps, and long analysis time, as well as their negative environmental impact, restrict their widespread use.[38] Alternatively, electrochemical methods, in particular electrochemical sensors, have received increasing attention owing to their high sensitivity, low cost, ease of handling, and short analysis time.[39−41] Various electrochemical sensors have been developed for 4-NP[17−19,42−49] and DA.[50−61] However, many of the developed electrochemical sensors for 4-NP and DA lack adequate selectivity and involve several and complicated preparation steps.

Herein, we report the development of an easily prepared, sensitive, cost-effective, and environmentally friendly voltammetric sensor for 4-NP and DA. The electrochemically activated GCE was utilized as a sensing platform for oxidizable (DA) and reducible (4-NP) analytes. The detailed response characteristics of AGCEs as sensors for DA and 4-NP, response

mechanisms, and analytical applications of the developed sensors are discussed below.

EXPERIMENTAL SECTION

Reagents. All chemicals were of analytical grade and used without further purification. Pyrocatechol, hydroquinone, and 2-aminophenol were purchased from SDFCL (India). 4-Nitrophenol was purchased from Merck. DA was obtained from Sigma. Na_2SO_4 was purchased from Koch-Light Laboratory Chemicals Ltd. (England). KI, $NiCl_2 \cdot 6H_2O$, and $CoCl_2$ were obtained from BDH Laboratory Chemicals Ltd. (England). Na_2HPO_4 and NaH_2PO_4 were purchased from ADWIC Laboratory Chemicals (Egypt). Phosphate-buffered saline supporting electrolyte (PBS, pH = 7.0) was prepared from NaH_2PO_4 (0.1 mol L^{-1}) and Na_2HPO_4 (0.1 mol L^{-1}).

Instruments. The interface 1000 Gamry electrochemical workstation was utilized in all electrochemical measurements. Such measurements were done using a three-electrode system. The working electrode was a bare GCE model MF-2012, 3.0 mm in diameter (Bioanalytical Systems), or an AGCE. Saturated double-junction Ag/AgCl and platinum wire were used as reference and counter electrodes, respectively. All experiments were performed at 25 ± 1 °C. DPV was performed with a pulse amplitude of 50 mV, a pulse width of 50 ms, and a pulse time of 200 ms. The scan rate was 50 mV/s.

Preparation of Activated Glassy Carbon Electrodes. The surface of the GCE was cleaned via polishing using 0.05 μm alumina slurry on a microcloth, followed by rinsing thoroughly with ethanol and double distilled water. To obtain the AGCE, the cleaned GCE was immersed in 0.1 M PBS (pH 7.0) and conditioned by CV between −1.5 and +2.5 V for five scans at a scan rate of 100 mV/s (see Scheme 1). After this electrochemical treatment, the AGCE was rinsed with double distilled water and stored in PBS for later use.

RESULTS AND DISCUSSION

Electrochemical Activation of GCEs. The electrochemical activation of the GCE surface was performed by successive CV (Scheme 1). Upon continuous scanning, a well-defined anodic peak (A) and cathodic peak (C) were observed at ∼ +1.5 and −0.65 V, respectively. Repetitive scans led to an
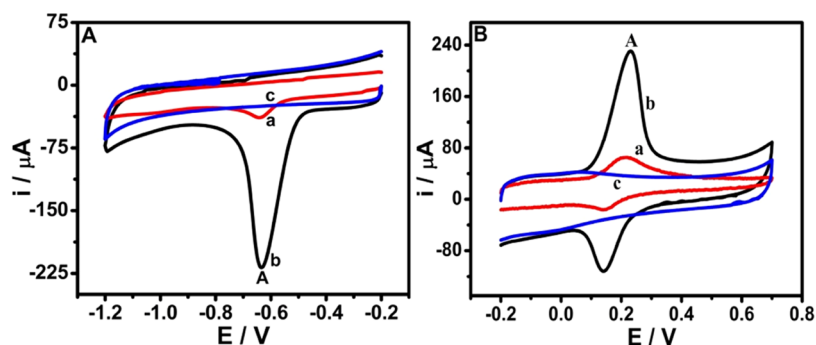
Figure 1. CVs of the bare GCE (a) and AGCE (b) in 0.1 M PBS (pH 7.0) containing 1×10^{-4} M 4-NP (A) and 5×10^{-4} M DA (B) at a scan rate of 100 mVs^{-1}. Curve (c) represents the CV of the AGCE in a blank solution (0.1 M PBS free from 4-NP and DA).
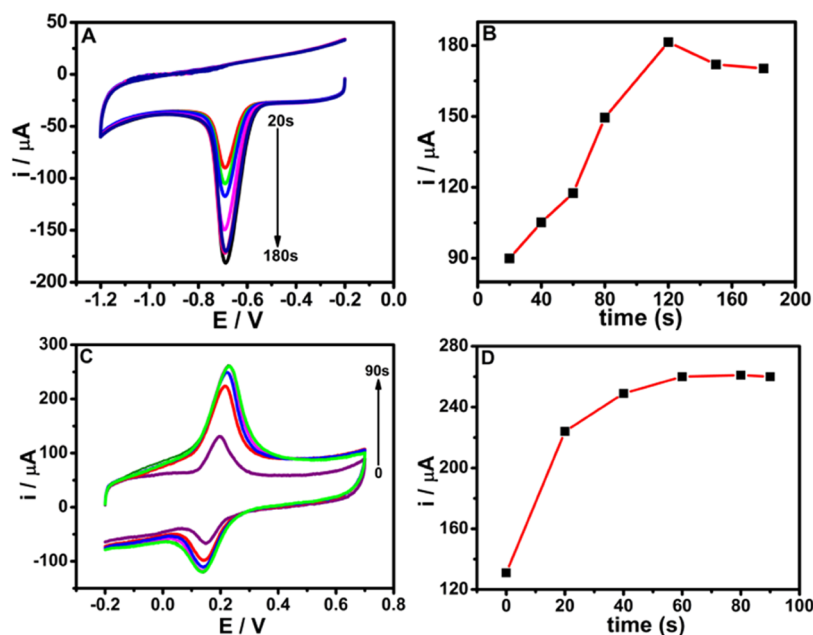

Figure 2. (A) CVs of 0.1 M PBS (pH 7.0) containing 1×10^{-4} M 4-NP at the AGCE as measured at different accumulation times (from 20 to 180s). (B) Effect of accumulation time on the cathodic peak currents of 4-NP. (C) CVs of 0.1 M PBS (pH 7.0) containing 5×10^{-4} M DA at the AGCE as measured at different accumulation times (from 0 to 90 s). (D) Effect of accumulation time on the anodic peak currents of DA.

increase in peak heights of A and C (Scheme 1). This behavior was well studied in our recent publication.[14] Combining a set of electrochemical and surface characterization techniques, we proved that the anodization of the GCE surface at a high voltage (2.5 V) leads to its surface activation with a concomitant formation of oxygen-containing surface functional groups (OxSFGs). Such OxSFGs are reduced in a well-defined cathodic process (peak C, Scheme 1).[14] The surface functionalization of the GCE resulted in a remarkable increase in adsorption active sites and effective surface area. In addition, OxSFGs enhance the electron transfer and the activity of the AGCE.

OxSFGs at the AGCE could account for the oxidation and reduction processes of various analytes. For instance, the surface phenolates and carboxylates could participate in the reduction of 4-NP as a reducible analyte. Other SFGs such as quinone, epoxide, and ketone could participate in the oxidation of DA (see Scheme 1). SFGs promote electron transfer to/ from target analytes at the AGCE surface, which results in an improvement of electron transfer kinetics and a remarkable increase in electrocatalytic activity.

Electrocatalytic Behaviors of 4-NP and DA at the AGCE. The electrochemical behaviors of 4-NP and DA were studied using CV. Figure 1 shows the CV responses of 1×10^{-4} M 4-NP (Figure 1A) and 5×10^{-4} M DA (Figure 1B) in 0.1 M PBS, pH 7.0, at the bare GCE (a) and AGCE (b). As seen in Figure 1A,B, very weak redox peaks were observed at the bare GCE compared to the AGCE. The small current response of the bare GCE toward 4-NP and DA could be attributed to weak adsorption and slow electron transfer at the electrode surface. A remarkable improvement in redox peak currents, however, is obtained for 4-NP and DA when the GCE was electrochemically activated to obtain the AGCE (curve b). This indicates that the electrochemical activation of the surface of the AGCE can facilitate the electron transfer at the electrode surface and enhance the adsorption of 4-NP and DA. The 5-fold enhancement of peak current (peak A) suggests that the AGCE remarkably enhances the electrocatalytic reduction of 4-NP and oxidation of DA. As previously mentioned, this enhancement could be attributed to the increase in effective surface area and the number of active sites, as well as the improvement of electron transfer ability and high electrocatalytic activity of the AGCE. The response of the
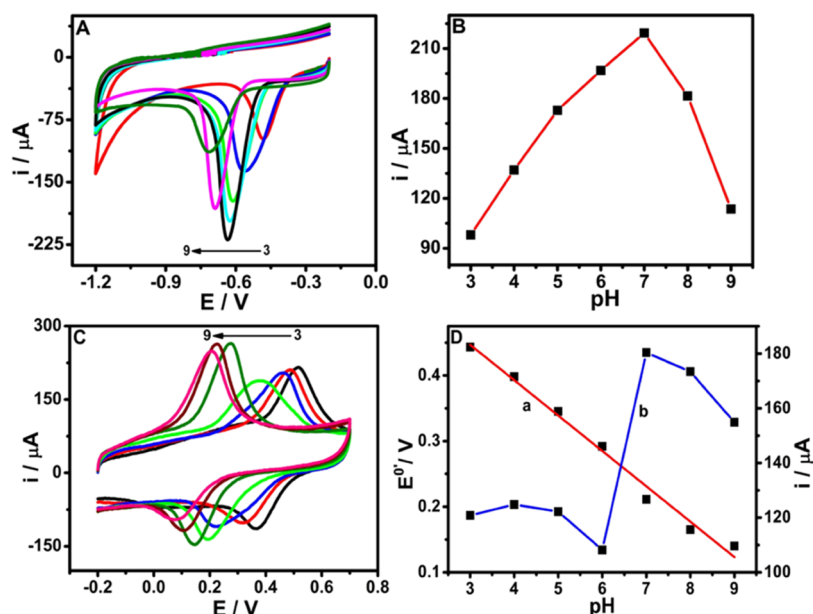
Figure 3. (A) CVs of 1×10^{-4} M 4-NP at the AGCE as measured at different pH values. (B) Relationship between pH and the cathodic peak currents of 4-NP. (C) CVs of 5×10^{-4} M DA at the AGCE as measured at different pH values. (D) Relationship between pH and the formal potential ($E^{0\prime}$) (a) and the relationship between pH and the anodic peak currents of DA (b).

AGCE in blank PBS was measured to ensure that peak (A) corresponds to the reduction of 4-NP and oxidation of DA (curve c). Indeed, in blank PBS (i.e., in the absence of 4-NP and DA), peak (A) was not observed, which indicates its correlation to 4-NP reduction and DA oxidation.

Optimization of the Voltammetric Response of the AGCE Toward 4-NP and DA. The effects of various parameters on the voltammetric responses of the AGCE toward 4-NP and DA were studied and optimized, including the pH of the supporting electrolyte, scan rate, and accumulation time. These parameters have a significant impact on the performance of the developed sensors, as detailed below.

Effect of Accumulation Time. Under an open-circuit potential, the accumulation of 4-NP and DA at the AGCE surface was investigated for various time intervals. The corresponding CVs were recorded (Figure 2A,C). The peak currents increased significantly from 20 to 120 s and from 0 to 60 s for 4-NP (Figure 2B) and DA (Figure 2D), respectively. This behavior indicates the enhancement of 4-NP and DA adsorption at the AGCE. Nevertheless, with a further increase in the accumulation time, the current practically reached a plateau, indicating that the active sites at the AGCE had been saturated. The observed accumulation time reveals the rapid adsorption of 4-NP and DA at the surface of the AGCE. To achieve the optimal AGCE performance (e.g., sensitivity and working efficiency), an accumulation time of 120 s for 4-NP and 60 s for DA was maintained throughout.

Effect of pH. The electrocatalytic behavior of 4-NP and DA is expected to be pH dependent because of proton involvement in the electrode reaction.[17,47,58,62] Subsequently, the effect of pH on the response of the AGCE toward 4-NP and DA in 0.1 M PBS was studied using CV in the pH range 3.0–9.0 (Figure 3A, C). In the case of 4-NP, the reduction peak current increased as the pH increased from 3.0 to 7.0 (Figure 3B). The peak current reached its maximum at pH 7.0 and then sharply decreased at higher pH values (see Figure 3B). This phenomenon could be explained based on the reduction

mechanism, which involves proton transfer[19,42,44,62] as described in Scheme 2. The participation of protons in the

Scheme 2. Reduction Mechanism of 4-NP at the AGCE
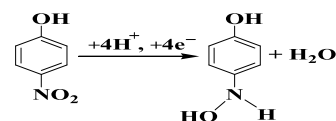
electrochemical reduction process is confirmed by the shift of the cathodic peak potentials negatively with increasing pH. At high hydroxyl ion concentrations, pH > 7, the reduction of the nitro group ($-NO_2$) of 4-NP to the hydroxylamine group ($-NHOH$) is retarded due to the decrease in H^+ concentration which participates in the reduction mechanism.[19,45,47,62] In addition, the percent of the anionic form of 4-NP (pK_a value of 7.2) increased with increasing pH.[47,62,63] Concomitantly, at alkaline pH, it is plausible that the OxSFGs deprotonate to their negatively charged forms. As a result, the electrostatic repulsion between 4-NP and the AGCE at alkaline pH might reduce the extent of its adsorption, which decreases the peak currents. Accordingly, pH 7.0 was chosen as the optimal pH value for detecting 4-NP.

Concerning DA, redox peak potentials are negatively shifted as the pH increases (Figure 3C). This shift reveals the direct participation of protons in the electrochemical redox processes.[57,64] A linear relationship was obtained between pH and formal potential ($E^{0\prime} = (E_{pa} + E_{pc})/2$) with a linear regression equation of $E^{0\prime} = (0.61 \pm 0.016) - (0.054 \pm 0.0026)$ pH ($R^2 = 0.986$) (Figure 3Da). The slope for this relationship, 54.0 mV/pH, is comparable to the theoretical value, 59.0 mV/pH. This observation suggests that an equal number of electrons and protons participate in the redox processes of DA.[52,55,57,64] As shown in Scheme 3, the redox process of DA involved two protons and two electrons transfer process related to the oxidation of DA to its quinonoid form and the subsequent reduction of the quinonoid form.[52,55,64] The peak

Scheme 3. Oxidation Mechanism of DA at the AGCE
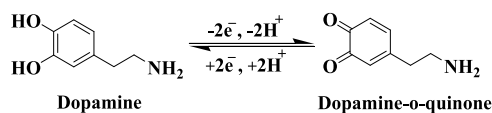
current reached its maximum at pH 7.0, and then the current gradually decreased at higher pH values (Figure 3D, b). At alkaline pH, OxSFGs at the AGCE could deprotonate to their negatively charged forms. Moreover, the percent of the cationic form of DA (pK_a = 8.9) is decreased with the increase in pH. Consequently, at high pH, the electrostatic attraction of DA to OxSFGs at the AGCE decreased. Both effects could participate in lowering DA adsorption at the AGCE and concomitantly reducing peak currents. Accordingly, pH 7.0, which is close to the physiological pH, was chosen as the optimal pH for detecting DA.

Effect of Scan Rate. Cyclic voltammetry was utilized to study the effect of scan rate (ν) on the response of the AGCE toward DA and 4-NP. CV experiments were performed at 1×10^{-4} M 4-NP (Figure 4A) and 5×10^{-4} M DA (Figure 4C) prepared in 0.1 M PBS, pH 7.0. Upon increasing the scan rate, a shift in peak potentials (E_p) and an increase in peak currents (i_p) were observed (Figure 4A,C). According to the Randles−Sevčik eq 1[65]

$$I_p = 2.69 \times 10^5 A \, n^{3/2} D_R^{1/2} c \, \nu^{1/2} \tag{1}$$

A plot of the peak current (I_p) versus the square root of scan rate ($\nu^{1/2}$) results in a linear relationship with linear regression equations of i_p (μA) = (-11.7 ± 3.52) + (25 ± 0.72) $\nu^{1/2}$ (mV/s)$^{1/2}$ (R = 0.994) for 4-NP (Figure 4B), and i_{pa} (μA) = (-12.2 ± 2.16) + (34.91 ± 1.12) $\nu^{1/2}$ (mV/s)$^{1/2}$ (R^2 = 0.991) for oxidation and i_{pa} (μA) = (19.7 ± 2.87) − (22.1 ± 1.32) $\nu^{1/2}$ (mV/s)$^{1/2}$ (R^2 = 0.976) for reduction for DA (Figure 4D), which could indicate a diffusion-controlled nature of the redox processes for both 4-NP[42,44,45,48,62] and DA.[51,58,59,64,66,67] The

shift in peak potential with the increase in scan rate may refer to the adsorption of analytes (DA or 4-NP) on the AGCE surface,[49] indicating the participation of both adsorption and diffusion in the redox mechanism.

Analytical Performance of the AGCE-Based 4-NP and DA Sensing Platform. DPVs were recorded to investigate the effect of increasing 4-NP and DA concentration on reduction peaks of 4-NP and oxidation peaks of DA. Under the optimized conditions, the linear ranges and LODs of 4-NP and DA at the optimized AGCE sensor were determined. The redox peak currents increased with increasing 4-NP (Figure 5A) or DA (Figure 5C) concentrations. It was observed that the peak current (i_p, μA) is proportional to the concentration of 4-NP (c, μM) over the concentration ranges from 0.04 to 65 and 65 to 370 μM, while from 0.02 to 1.0 and 1.0 to 100 μM for DA. The corresponding calibration plots show a linear relationship with linear regression equations of i_p (μA) = (1.05 $\pm$ 0.26) + (1.3 $\pm$ 0.043) c (μM) (R^2 = 0.995), i_p (μA) = (68.4 $\pm$ 2.79) + (0.2 $\pm$ 0.01) c (μM) (R^2 = 0.984) for 4-NP (Figure 5B) and i_p (μA) = (4.2 $\pm$ 0.42) + (35.59 $\pm$ 1.29) c (μM) (R^2 = 0.994), i_p (μA) = (43.01 $\pm$ 2.82) + (0.91 $\pm$ 0.056) c (μM) (R^2 = 0.981) for DA (Figure 5D). In addition, the LODs were found to be 0.02 and 0.01 μM (S/N = 3) for 4-NP and DA, respectively.

Repeatability, Stability, and Interference Studies. The repeatability of AGCEs was investigated by performing 10 replicate measurements in 100 μM 4-NP or 50 μM DA. The relative standard deviation (R.S.D) was found to be 3.4 and 1.1% for 4-NP and DA, respectively. Such R.S.D values indicate excellent repeatability of the AGCEs.

The current responses of the AGCE toward 100 μM 4-NP prepared in 0.1 M PBS (pH 7.0) were measured for 1 week. As shown in Figure S1, the electrochemical responses of the AGCE were found to be practically stable for 5 days with a signal change of about 3.0%. Thereafter, the current responses
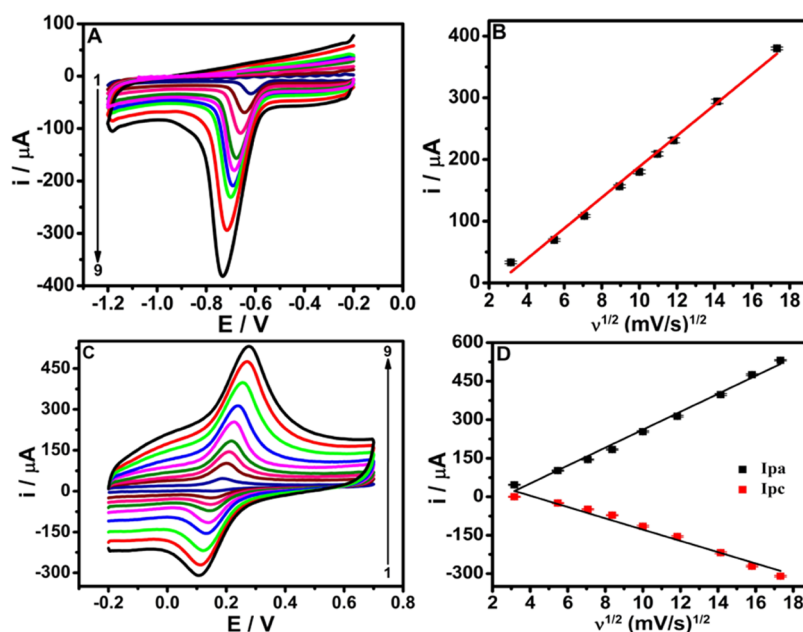

Figure 4. (A) CVs of the AGCE at different scan rates in 0.1 M PBS (pH 7.0) containing 1×10^{-4} M 4-NP (A) and 5×10^{-4} M DA (C). Scan rates from 10 to 300 mVs^{-1}. (B) Plot of the cathodic peak current (i_p) of 4-NP versus the square root of the scan rate ($\nu^{1/2}$). (D) Plots of the anodic peak current (i_{pa}) and cathodic peak current (i_{pc}) of DA versus the square root of the scan rate ($\nu^{1/2}$).
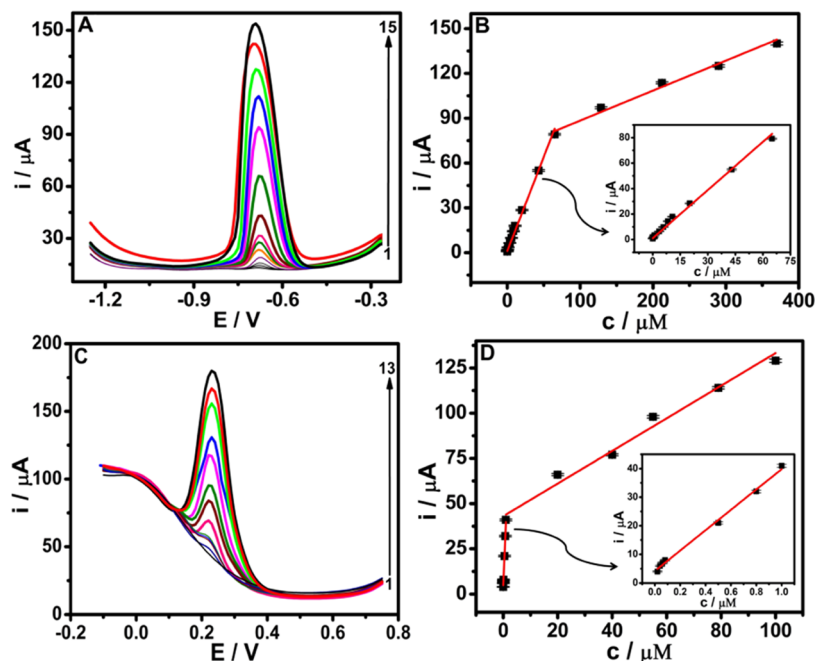
Figure 5. (A) DPVs of different concentrations of 4-NP as measured in 0.1 M PBS, pH 7.0, at the AGCE. Concentrations (from 1 to 15): 0.04, 0.08, 0.52, 1.0, 3.5, 5.8, 8.3, 10.7, 20.2, 43.0, 65.0, 128.74, 212.3, 290.0, and 370.0 μM. (B) Corresponding calibration plot for 4-NP at the AGCE. (C) DPVs of different concentrations of DA as measured in 0.1 M PBS, pH 7.0, at the AGCE. Concentrations (from 1 to 13): 0, 0.02, 0.04, 0.06, 0.08, 0.5, 0.8, 1.0, 20.0, 40.0, 55.0, 79.0, and 100.0 μM. (D) Corresponding calibration plot for DA at the AGCE. The inset of (D) indicates the responses at low concentrations of DA.

of the AGCE toward 4-NP decreased, which indicates reasonable stability of the developed sensor.

Potential interferents, which are reduced or oxidized at the same potential windows of 4-NP and DA, respectively, represent the main threat to the developed sensing platform when applied for the analysis of real samples.

The selectivity of the AGCE-based 4-NP sensor was examined by the addition of interferents to a 100 μM 4-NP solution. Results obtained indicated that 10-fold of catechol (CC), hydroquinone (HQ), 2-aminophenol (2-AP), 4-chlorophenol (4-CP), and chlorpyrifos (Chpy) (Figure S2) and 500-fold of Na$^+$, K$^+$, Co^{2+}, Ni^{2+}, I$^-$, Cl$^-$, and SO$_4^{2-}$ did not practically affect the detection of 4-NP (signal change below 5%) (see data depicted in Table S1).

Ascorbic acid (AA) is the main coexisting interferent in real biological samples. Therefore, the selectivity of the AGCE toward DA in the presence of AA must be given high consideration. The DPV current responses of the AGCE toward DA were examined by the addition of AA to 50 μM DA. Results obtained indicated that 40-fold of AA did not practically affect the DPV peak currents of DA (see Figure S3) (signal change below 5%). This data reveals that the optimized AGCE-based DA sensor has an acceptable tolerance level against AA (see data depicted in Table S2). The observed selectivity of the proposed sensor for DA relative to AA could be explained by strong electrostatic attraction between the NH$_3^+$ groups of DA (pK_a = 8.9) and the negatively charged OxSFGs at pH 7.0 (see above). On the other hand, AA, with a pKa value of 4.1, is fully deprotonated to its anionic form at pH 7.0.[64] Thus, the strong electrostatic repulsion between AA and the negatively charged OxSFGs is expected to reduce the adsorption of AA and consequently lower its peak current.

The selectivity of the AGCE sensing platform toward DA in the presence of other common interferents, such as uric acid (UA) and folic acid (FA), was also investigated. Results obtained indicated that 50-fold of UA and FA did not practically affect the detection of 5 μM DA (signal change below 5%) (see Figure S4).

These findings suggest that the AGCE sensing platform has a high selectivity for 4-NP and DA and could be used as a reliable and cost-effective sensing platform for selective detection of 4-NP and DA in real samples.

Analytical Applications of AGCE-Based 4-NP and DA Sensors. To demonstrate the analytical utility of the AGCE-based 4-NP sensor, various environmental water samples including tap water, Nile river water, and wastewater were tested using spiking and recovery experiments. As shown in Table 1, an average recovery of 96.5% was observed. Moreover,

Table 1. Results for Spiking and Recovery Analysis of 4-NP in Water Samples Using the AGCE-Based Sensing Platform

sample	added (μM)	detected (μM)	recovery (%)	RSD (%, n = 3)
tab water	1.0	0.93	93	5
Nile river	2.0	1.94	97	3
wastewater 1	3.0	3.03	101	2
wastewater 2	4.0	3.80	95	3

the analytical utility of the AGCE sensing platform for DA was investigated by testing three human urine samples using spiking and recovery experiments. Fresh urine samples were diluted in a ratio of 1:100 using PBS, pH 7.0. Then, the diluted urine samples were spiked with a known concentration of DA prior to DPV measurements. Results obtained revealed an average recovery of 98.0%, demonstrating satisfactory recovery results for the AGCE sensing platform (see data depicted in Table 2).

Table 2. Results for Spiking and Recovery Analysis of DA in Human Urine Samples Using the AGCE-Based Sensing Platform

sample	spiked (μM)	found (μM)	recovery (%)	RSD (%, n = 3)
1	5.0	4.80	96	3
2	10.0	10.2	102	4
3	15.0	14.3	95	4

Comparison of the Proposed AGCE-Based Sensor with Different Modified Electrodes for 4-NP and DA. In comparison with the previously reported 4-NP (Table S3) and DA (Table S4) electrochemical sensors, the optimized AGCE-based 4-NP and DA sensor showed high sensitivity, wide linear ranges, and low detection limits compared to most of the previously reported electrochemical sensors (Tables S3 and S4). In particular, the developed DA sensor is characterized by much higher sensitivity ($\sim$504 μA μM^{-1} cm^{-2}) and a lower detection limit compared to all reported electrochemical sensors (see Table S4). Moreover, the developed sensors are characterized by low cost and operational simplicity since there is no complicated modification procedure required for surface modification of the GCE.

CONCLUSIONS

An electrochemically activated GCE, possessing OxSFGs, was proven to be a useful sensing platform for both reducible (e.g., 4-NP) and oxidizable (e.g., DA) analytes. The AGCE sensing platform was utilized for the development of simple, sensitive, selective, and easily fabricated sensors for the determination of 4-NP and DA by differential pulse voltammetry (DPV). Because of its high electrocatalytic activity, excellent repeatability, and high sensitivity, the AGCE sensing platform can be used for routine analysis of 4-NP and DA in real samples. Under optimized conditions, the developed AGCE-based 4-NP sensor exhibited linear ranges of 0.04−65 and 65−370 μM with a detection limit as low as 0.02 μM. Moreover, the developed sensor exhibited a linear response over the concentration ranges of 0.02−1.0 and 1.0−100 μM with a lower limit of detection (LOD) of 0.01 μM (S/N = 3) for DA. The developed sensors were successfully utilized to detect 4-NP and DA in different real samples with satisfactory results.

ASSOCIATED CONTENT

ⓢ Supporting Information

The Supporting Information is available free of charge at https://pubs.acs.org/doi/10.1021/acsomega.2c03427.

> Lifetime of the AGCE-based sensor platform; effect of addition of 1.0×10^{-3} M CC, HQ, 2-AP, 4-CP, or Chpy on AGCE DPV responses of AGCE towards 1.0×10^{-4} M 4-NP; study of the effect of some interferents on the peak current response of the AGCE toward 1.0×10^{-4} M 4-NP; effect of the addition of different AA concentrations on the AGCE DPV responses toward 5 $\times 10^{-5}$ M DA; percent changes in AGCE DPV response toward 5 $\times 10^{-5}$ M DA in the presence of different concentrations of AA; effect of 50-fold addition of UA or folic acid on the AGCE DPV response toward 5 $\times 10^{-6}$ M DA; analytical features of different electrochemical sensors for the assay of 4-NP using the DPV technique; and analytical features of different electrochemical sensors for the assay of DA (PDF)

■ AUTHOR INFORMATION

Corresponding Author

Ibrahim H. A. Badr − *Chemistry Department, Faculty of Science, Ain-Shams University, Cairo 11566, Egypt; Department of Chemistry, Faculty of Science, Galala University, Suez 43511, Egypt;* ⓘ orcid.org/0000-0003-1683-3827; Email: ihbadr@sci.asu.edu.eg, ibrahim.badr@gu.edu.eg

Authors

Ali M. Abdel-Aziz − *Chemistry Department, Faculty of Science, Ain-Shams University, Cairo 11566, Egypt;* ⓘ orcid.org/0000-0002-8913-3816

Hamdy H. Hassan − *Chemistry Department, Faculty of Science, Ain-Shams University, Cairo 11566, Egypt; Department of Chemistry, Faculty of Science, Galala University, Suez 43511, Egypt*

Complete contact information is available at:
https://pubs.acs.org/10.1021/acsomega.2c03427

Notes

The authors declare no competing financial interest.

■ REFERENCES

(1) Craievich, A. On the structure of glassy carbon. *Mater. Res. Bull.* **1976**, *11*, 1249−1255.

(2) Jenkins, G. M.; Kawamura, K. Structure of glassy carbon. *Nature* **1971**, *231*, 175.

(3) Fagan, D. T.; Hu, I. F.; Kuwana, T. Vacuum heat-treatment for activation of glassy carbon electrodes. *Anal. Chem.* **1985**, *57*, 2759−2763.

(4) Bowling, R. J.; Packard, R. T.; McCreery, R. L. Activation of highly ordered pyrolytic graphite for heterogeneous electron transfer: relationship between electrochemical performance and carbon microstructure. *J. Am. Chem. Soc.* **1989**, *111*, 1217−1223.

(5) Kamau, G. N.; Willis, W. S.; Rusling, J. F. Electrochemical and electron spectroscopic studies of highly polished glassy carbon electrodes. *Anal. Chem.* **1985**, *57*, 545−551.

(6) Zhang, H.; Coury, L. A. Effects of high-intensity ultrasound on glassy carbon electrodes. *Anal. Chem.* **1993**, *65*, 1552−1558.

(7) Upadhyay, P. A simple procedure for activating a glassy carbon electrode. *J. Electroanal. Chem. Interfacial Electrochem.* **1989**, *271*, 339−343.

(8) Engstrom, R. C. Electrochemical pretreatment of glassy carbon electrodes. *Anal. Chem.* **1982**, *54*, 2310−2314.

(9) Engstrom, R. C.; Strasser, V. A. Characterization of electrochemically pretreated glassy carbon electrodes. *Anal. Chem.* **1984**, *56*, 136−141.

(10) Nagaoka, T.; Yoshino, T. Surface properties of electrochemically pretreated glassy carbon. *Anal. Chem.* **1986**, *58*, 1037−1042.

(11) Kepley, L. J.; Bard, A. J. Ellipsometric, electrochemical, and elemental characterization of the surface phase produced on glassy carbon electrodes by electrochemical activation. *Anal. Chem.* **1988**, *60*, 1459−1467.

(12) Ilangovan, G.; Chandrasekara Pillai, K. Electrochemical and XPS characterization of glassy carbon electrode surface effects on the preparation of a monomeric molybdate (VI)-modified electrode. *Langmuir* **1997**, *13*, 566−575.

(13) Ilangovan, G.; Pillai, K. C. Unusual activation of glassy carbon electrodes for enhanced adsorption of monomeric molybdate (VI). *J. Electroanal. Chem.* **1997**, *431*, 11−14.

(14) Abdel-Aziz, A. M.; Hassan, H. H.; Badr, I. H. A. Glassy Carbon Electrode Electromodification in the Presence of Organic Monomers: Electropolymerization versus Activation. *Anal. Chem.* **2020**, *92*, 7947−7954.

(15) Pan, B.; Chen, X.; Pan, B.; Zhang, W.; Zhang, X.; Zhang, Q. Preparation of an aminated macroreticular resin adsorbent and its adsorption of p-nitrophenol from water. *J. Hazard. Mater.* **2006**, *137*, 1236−1240.

(16) He, Q.; Tian, Y.; Wu, Y.; Liu, J.; Li, G.; Deng, P.; Chen, D. Facile and Ultrasensitive Determination of 4-Nitrophenol Based on Acetylene Black Paste and Graphene Hybrid Electrode. *Nanomaterials* **2019**, *9*, 429.

(17) Peng, D.; Zhang, J.; Qin, D.; Chen, J.; Shan, D.; Lu, X. An electrochemical sensor based on polyelectrolyte-functionalized graphene for detection of 4-nitrophenol. *J. Electroanal. Chem.* **2014**, *734*, 1−6.

(18) Zhang, J.; Cui, S.; Ding, Y.; Yang, X.; Guo, K.; Zhao, J.-T. Two-dimensional mesoporous ZnCo2O4 nanosheets as a novel electrocatalyst for detection of o-nitrophenol and p-nitrophenol. *Biosens. Bioelectron.* **2018**, *112*, 177−185.

(19) Zeng, Y.; Zhou, Y.; Zhou, T.; Shi, G. A novel composite of reduced graphene oxide and molecularly imprinted polymer for electrochemical sensing 4-nitrophenol. *Electrochim. Acta* **2014**, *130*, 504−511.

(20) Doğan, H. Ö.; Urhan, B. K.; Çepni, E.; Eryiğit, M. Simultaneous electrochemical detection of ascorbic acid and dopamine on Cu2O/CuO/electrochemically reduced graphene oxide (CuxO/ERGO)-nanocomposite-modified electrode. *Microchem. J.* **2019**, *150*, No. 104157.

(21) Tajik, S.; Beitollahi, H.; Aflatoonian, M. R. A novel dopamine electrochemical sensor based on La3+/ZnO nanoflower modified graphite screen printed electrode. *J. Electrochem. Sci. Eng.* **2019**, *9*, 187−195.

(22) Hou, F.; Deng, T.; Jiang, X. Dispersive liquid-liquid microextraction of phenolic compounds using solidified floating organic droplets, and their determination by HPLC. *Microchim. Acta* **2013**, *180*, 341−346.

(23) Liu, X.; Ji, Y.; Zhang, Y.; Zhang, H.; Liu, M. Oxidized multiwalled carbon nanotubes as a novel solid-phase microextraction fiber for determination of phenols in aqueous samples. *J. Chromatogr. A* **2007**, *1165*, 10−17.

(24) Karimi, M.; Carl, J. L.; Loftin, S.; Perlmutter, J. S. Modified high-performance liquid chromatography with electrochemical detection method for plasma measurement of levodopa, 3-O-methyldopa, dopamine, carbidopa and 3, 4-dihydroxyphenyl acetic acid. *J. Chromatogr. B* **2006**, *836*, 120−123.

(25) Naccarato, A.; Gionfriddo, E.; Sindona, G.; Tagarelli, A. Development of a simple and rapid solid phase microextraction-gas chromatography—triple quadrupole mass spectrometry method for the analysis of dopamine, serotonin and norepinephrine in human urine. *Anal. Chim. Acta* **2014**, *810*, 17−24.

(26) Liu, J.; Chen, H.; Lin, Z.; Lin, J.-M. Preparation of surface imprinting polymer capped Mn-doped ZnS quantum dots and their application for chemiluminescence detection of 4-nitrophenol in tap water. *Anal. Chem.* **2010**, *82*, 7380−7386.

(27) Hao, T.; Wei, X.; Nie, Y.; Xu, Y.; Yan, Y.; Zhou, Z. An eco-friendly molecularly imprinted fluorescence composite material based on carbon dots for fluorescent detection of 4-nitrophenol. *Microchim. Acta* **2016**, *183*, 2197−2203.

(28) Duan, H.; Li, L.; Wang, X.; Wang, Y.; Li, J.; Luo, C. A sensitive and selective chemiluminescence sensor for the determination of dopamine based on silanized magnetic graphene oxide-molecularly imprinted polymer. *Spectrochim. Acta, Part A* **2015**, *139*, 374−379.

(29) Toral, M. I.; Beattie, A.; Santibañez, C.; Richter, P. Simultaneous determination of parathion and p-nitrophenol in vegetable tissues by derivative spectrophotometry. *Environ. Monit. Assess.* **2002**, *76*, 263−274.

(30) Mamiński, M.; Olejniczak, M.; Chudy, M.; Dybko, A.; Brzózka, Z. Spectrophotometric determination of dopamine in microliter scale using microfluidic system based on polymeric technology. *Anal. Chim. Acta* **2005**, *540*, 153−157.

(31) Fang, H.; Pajski, M. L.; Ross, A. E.; Venton, B. J. Quantitation of dopamine, serotonin and adenosine content in a tissue punch from a brain slice using capillary electrophoresis with fast-scan cyclic voltammetry detection. *Anal. Methods* **2013**, *5*, 2704−2711.

(32) Dutta, P.; Pernites, R. B.; Danda, C.; Advincula, R. C. SPR detection of dopamine using cathodically electropolymerized, molecularly imprinted poly-p-aminostyrene thin films. *Macromol. Chem. Phys.* **2011**, *212*, 2439−2451.

(33) Qian, C.-G.; Zhu, S.; Feng, P.-J.; Chen, Y.-L.; Yu, J.-C.; Tang, X.; Liu, Y.; Shen, Q.-D. Conjugated polymer nanoparticles for fluorescence imaging and sensing of neurotransmitter dopamine in living cells and the brains of zebrafish larvae. *ACS Appl. Mater. Interfaces* **2015**, *7*, 18581−18589.

(34) Wang, H.-B.; Li, Y.; Bai, H.-Y.; Liu, Y.-M. Fluorescent determination of dopamine using polythymine-templated copper nanoclusters. *Anal. Lett.* **2018**, *51*, 2868−2877.

(35) Wang, H.-B.; Li, Y.; Dong, G.-L.; Gan, T.; Liu, Y.-M. A convenient and label-free colorimetric assay for dopamine detection based on the inhibition of the Cu (ii)-catalyzed oxidation of a 3, 3′, 5, 5′-tetramethylbenzidine−H 2 O 2 system. *New J. Chem.* **2017**, *41*, 14364−14369.

(36) Wang, H.-B.; Tao, B.-B.; Wu, N.-N.; Zhang, H.-D.; Liu, Y.-M. Glutathione-stabilized copper nanoclusters mediated-inner filter effect for sensitive and selective determination of p-nitrophenol and alkaline phosphatase activity. *Spectrochim. Acta, Part A* **2022**, *271*, No. 120948.

(37) Wang, H.-B.; Zhang, H.-D.; Chen, Y.; Huang, K.-J.; Liu, Y.-M. A label-free and ultrasensitive fluorescent sensor for dopamine detection based on double-stranded DNA templated copper nano-particles. *Sens. Actuators, B* **2015**, *220*, 146−153.

(38) Diab, N.; Morales, D. M.; Andronescu, C.; Masoud, M.; Schuhmann, W. A sensitive and selective graphene/cobalt tetrasulfonated phthalocyanine sensor for detection of dopamine. *Sens. Actuators, B* **2019**, *285*, 17−23.

(39) Badr, I. H. A.; Hassan, H. H.; Hamed, E.; Abdel-Aziz, A. M. Sensitive and Green Method for Determination of Chemical Oxygen Demand Using a Nano-copper Based Electrochemical Sensor. *Electroanalysis* **2017**, *29*, 2401−2409.

(40) Hassan, H. H.; Badr, I. H.; Abdel-Fatah, H. T.; Elfeky, E. M.; Abdel-Aziz, A. M. Low cost chemical oxygen demand sensor based on electrodeposited nano-copper film. *Arabian J. Chem.* **2018**, *11*, 171−180.

(41) Abdel-Aziz, A. M.; Hassan, H. H.; Hassan, A. A.; Badr, I. H. A Sensitive and Green Method for Determination of Catechol Using Multi-Walled Carbon Nanotubes/Poly (1, 5-diaminonaphthalene) Composite Film Modified Glassy Carbon Electrode. *J. Electrochem. Soc.* **2019**, *166*, B1441−B1451.

(42) Thirumalraj, B.; Rajkumar, C.; Chen, S.-M.; Lin, K.-Y. Determination of 4-nitrophenol in water by use of a screen-printed carbon electrode modified with chitosan-crafted ZnO nanoneedles. *J. Colloid Interface Sci.* **2017**, *499*, 83−92.

(43) Giribabu, K.; Haldorai, Y.; Rethinasabapathy, M.; Jang, S.-C.; Suresh, R.; Cho, W.-S.; Han, Y.-K.; Roh, C.; Huh, Y. S.; Narayanan, V. Glassy carbon electrode modified with poly (methyl orange) as an electrochemical platform for the determination of 4-nitrophenol at nanomolar levels. *Curr. Appl. Phys.* **2017**, *17*, 1114−1119.

(44) Zhang, T.; Lang, Q.; Yang, D.; Li, L.; Zeng, L.; Zheng, C.; Li, T.; Wei, M.; Liu, A. Simultaneous voltammetric determination of nitrophenol isomers at ordered mesoporous carbon modified electrode. *Electrochim. Acta* **2013**, *106*, 127−134.

(45) Deng, P.; Xu, Z.; Li, J. Simultaneous voltammetric determination of 2-nitrophenol and 4-nitrophenol based on an acetylene black paste electrode modified with a graphene-chitosan composite. *Microchim. Acta* **2014**, *181*, 1077−1084.

(46) Rao, H.; Guo, W.; Hou, H.; Wang, H.; Yin, B.; Xue, Z.; Zhao, G. Electroanalytical investigation of p-nitrophenol with dual electro-active groups on a reduced graphene oxide modified glassy carbon electrode. *Int. J. Electrochem. Sci.* **2017**, *12*, 1052−1063.

(47) Wei, T.; Huang, X.; Zeng, Q.; Wang, L. Simultaneous electrochemical determination of nitrophenol isomers with the polyfurfural film modified glassy carbon electrode. *J. Electroanal. Chem.* **2015**, *743*, 105−111.

(48) Balasubramanian, P.; Balamurugan, T.; Chen, S.-M.; Chen, T.-W. Simplistic synthesis of ultrafine CoMnO3 nanosheets: An excellent electrocatalyst for highly sensitive detection of toxic 4-nitrophenol in environmental water samples. *J. Hazard. Mater.* **2019**, *361*, 123−133.

(49) Sajjan, V. A.; Aralekallu, S.; Nemakal, M.; Palanna, M.; Prabhu, C. K.; Sannegowda, L. K. Nanomolar detection of 4-nitrophenol using Schiff-base phthalocyanine. *Microchem. J.* **2021**, *164*, No. 105980.

(50) Yue, H. Y.; Wu, P. F.; Huang, S.; Wang, Z. Z.; Gao, X.; Song, S. S.; Wang, W. Q.; Zhang, H. J.; Guo, X. R. Golf ball-like MoS 2 nanosheet arrays anchored onto carbon nanofibers for electrochemical detection of dopamine. *Microchim. Acta* **2019**, *186*, No. 378.

(51) Yang, H.; Zhao, J.; Qiu, M.; Sun, P.; Han, D.; Niu, L.; Cui, G. Hierarchical bi-continuous Pt decorated nanoporous Au-Sn alloy on carbon fiber paper for ascorbic acid, dopamine and uric acid simultaneous sensing. *Biosens. Bioelectron.* **2019**, *124−125*, 191−198.

(52) Venkataprasad, G.; Reddy, T. M.; Narayana, A. L.; Hussain, O.; Shaikshavali, P.; Gopal, T. V.; Gopal, P. A facile synthesis of Fe3O4-Gr nanocomposite and its effective use as electrochemical sensor for the determination of dopamine and as anode material in lithium ion batteries. *Sens. Actuators, A* **2019**, *293*, 87−100.

(53) Su, S.; Hao, Q.; Yan, Z.; Dong, R.; Yang, R.; Zhu, D.; Chao, J.; Zhou, Y.; Wang, L. A molybdenum disulfide@ Methylene Blue nanohybrid for electrochemical determination of microRNA-21, dopamine and uric acid. *Microchim. Acta* **2019**, *186*, No. 607.

(54) Song, H.; Zhao, H.; Zhang, X.; Xu, Y.; Cheng, X.; Gao, S.; Huo, L. A hollow urchin-like α-MnO 2 as an electrochemical sensor for hydrogen peroxide and dopamine with high selectivity and sensitivity. *Microchim. Acta* **2019**, *186*, No. 210.

(55) Ma, B.; Guo, H.; Wang, M.; Li, L.; Jia, X.; Chen, H.; Xue, R.; Yang, W. Electrocatalysis of Cu− MOF/Graphene Composite and its Sensing Application for Electrochemical Simultaneous Determination of Dopamine and Paracetamol. *Electroanalysis* **2019**, *31*, 1002−1008.

(56) Ma, L.; Zhang, Q.; Wu, C.; Zhang, Y.; Zeng, L. PtNi bimetallic nanoparticles loaded MoS2 nanosheets: Preparation and electrochemical sensing application for the detection of dopamine and uric acid. *Anal. Chim. Acta* **2019**, *1055*, 17−25.

(57) Huang, Z.-N.; Zou, J.; Teng, J.; Liu, Q.; Yuan, M.-M.; Jiao, F.-P.; Jiang, X.-Y.; Yu, J.-G. A novel electrochemical sensor based on self-assembled platinum nanochains-multi-walled carbon nanotubes-graphene nanoparticles composite for simultaneous determination of dopamine and ascorbic acid. *Ecotoxicol. Environ. Saf.* **2019**, *172*, 167−175.

(58) Feng, J.; Li, Q.; Cai, J.; Yang, T.; Chen, J.; Hou, X. Electrochemical detection mechanism of dopamine and uric acid on titanium nitride-reduced graphene oxide composite with and without ascorbic acid. *Sens. Actuators, B* **2019**, *298*, No. 126872.

(59) Liu, X.; Xi, X.; Chen, C.; Liu, F.; Wu, D.; Wang, L.; Ji, W.; Su, Y.; Liu, R. Ordered mesoporous carbon-covered carbonized silk fabrics for flexible electrochemical dopamine detection. *J. Mater. Chem. B* **2019**, *7*, 2145−2150.

(60) Prabhu, C. K.; Nemakal, M.; Aralekallu, S.; Mohammed, I.; Palanna, M.; Sajjan, V. A.; Akshitha, D.; Sannegowda, L. K. A comparative study of carboxylic acid and benzimidazole phthalocyanines and their surface modification for dopamine sensing. *J. Electroanal. Chem.* **2019**, *847*, No. 113262.

(61) Sajjan, V. A.; Mohammed, I.; Nemakal, M.; Aralekallu, S.; Kumar, K. H.; Swamy, S.; Sannegowda, L. K. Synthesis and electropolymerization of cobalt tetraaminebenzamidephthalocyanine macrocycle for the amperometric sensing of dopamine. *J. Electroanal. Chem.* **2019**, *838*, 33−40.

(62) Ghazizadeh, A. J.; Afkhami, A.; Bagheri, H. Voltammetric determination of 4-nitrophenol using a glassy carbon electrode modified with a gold-ZnO-SiO 2 nanostructure. *Microchim. Acta* **2018**, *185*, No. 296.

(63) Ikhsan, N. I.; Rameshkumar, P.; Huang, N. M. Controlled synthesis of reduced graphene oxide supported silver nanoparticles for selective and sensitive electrochemical detection of 4-nitrophenol. *Electrochim. Acta* **2016**, *192*, 392−399.

(64) Li, X.-B.; Rahman, M. M.; Xu, G.-R.; Lee, J.-J. Highly sensitive and selective detection of dopamine at poly (chromotrope 2B)-modified glassy carbon electrode in the presence of uric acid and ascorbic acid. *Electrochim. Acta* **2015**, *173*, 440−447.

(65) Bard, A. J.; Faulkner, L. R. *Electrochemical Methods: Fundamentals and Applications*, 2nd ed.; Wiley: New York, 2001.

(66) Wu, F.; Huang, T.; Hu, Y.; Yang, X.; Ouyang, Y.; Xie, Q. Differential pulse voltammetric simultaneous determination of ascorbic acid, dopamine and uric acid on a glassy carbon electrode modified with electroreduced graphene oxide and imidazolium groups. *Microchim. Acta* **2016**, *183*, 2539−2546.

(67) Gao, F.; Cai, X.; Wang, X.; Gao, C.; Liu, S.; Gao, F.; Wang, Q. Highly sensitive and selective detection of dopamine in the presence of ascorbic acid at graphene oxide modified electrode. *Sens. Actuators, B* **2013**, *186*, 380−387.